ACRS 2022
MONGOLIA

EFFECTS OF LANDSAT DATA COLLECTION LEVEL ON ESTIMATION OF THE CHLOROPHYLL-A CONCENTRATION

Yoshinari Oguro[1], Tomohisa Konishi[2], Seiji Ito[3] and Chiemi Miura[4]
[1]Hiroshima Institute of Technology, 2-1-1 Miyake, Saeki-ku, Hiroshima 731-5193, Japan,
Email: y.oguro.yx@it-hiroshima.ac.jp
[2]Hiroshima Institute of Technology, 2-1-1 Miyake, Saeki-ku, Hiroshima 731-5193, Japan,
Email: t.konishi.vd@it-hiroshima.ac.jp
[3]Hiroshima Institute of Technology, 2-1-1 Miyake, Saeki-ku, Hiroshima 731-5193, Japan,
Email: s.itoh.us@it-hiroshima.ac.jp
[4]Hiroshima Institute of Technology, 2-1-1 Miyake, Saeki-ku, Hiroshima 731-5193, Japan,
Email: c.miura.6u@it-hiroshima.ac.jp

KEY WORDS: Landsat Collection 1 Level-1 data, Landsat Collection 2 Level-1 data, Biological-optical model

ABSTRACT: Uwa Sea located of Uwajima City and Ainan Town of Ehime Prefecture in Japan are very famous places for the birthplace of a pearl. By a pearl farming, it is very important to grasp marine information correctly of the Chlorophyll-a concentration and the Seawater Temperature etc. We have been previously studied an estimation method of the Chlorophyll-a concentrations for the Landsat Collection 1 Level-1 (C1-L1) data via the linear combination index (LCI) proposed by Robert Frouin et al.(2006). On the other hand, the Landsat Collection 2 data distribution process was start on December in 2020, and this data improvements for the geometric and radiometric quality. Moreover, the Landsat Collection 1 data will end on December 31, 2022. Therefore, we investigated the effects of differences in the Landsat Collection Levels between the C1-L1 data and the C2-L1 data on estimation of Chlorophyll-a concentration. First, we compared the Chlorophyll-a concentration by the water quality survey data at Uwa Sea and that of the estimated values by the Landsat-8/OLI data of both collections (C1-L1 and C2-L1). As a result, the C1-L1 data and the C2-L1 data yielded similar estimate and it was confirmed that compatibility between the two collections. Secondly, the estimated formula of the Landsat-8/OLI data was corrected so that it can correspond to a wide range of 0.1-10 mg/m3 of the Chlorophyll-a concentrations using a simulation with the bio-optical model proposed by Andre Morel et al. (2001) since the range of the Chlorophyll-a concentration measured in Uwa Sea is very narrow of 0.37–1.33 mg/m^3. As a result, we found that the root-mean-squared (RMS) error of 12.4% and 9.4% in the range of Chlorophyll-a concentration 0.3–10 mg/m^3 for the C1-L1 data and C2-L1 data, respectively.

1. INTRODUCTION

Ehime Prefecture in Japan are very famous places for the birthplace of pearls, and the account for about 42% of Japan's pearl production. The pearls are farmed and produced mainly Uwa Sea located of Uwajima City and Ainan Town of Ehime Prefecture. By a pearl farming, it is very important to grasp marine information correctly of the Chlorophyll-a (Chl.a) concentration and the Seawater Temperature etc. Especially, the nutrients such as the Chl.a concentrations are very important marine information in pearl farming. On the other hand, there are various methods for the Chl.a analysis using satellite data. Here, it is known that the estimating method of the Chl.a concentration via the linear combination index (LCI) proposed by Robert Frouin et al.(2006) can mitigate the atmospheric influence to some extent (Sakuno, 2013, Oguro, 2021). Previously, we have been studied an estimation method of the Chl.a concentrations for the Landsat Collection 1 Level-1 (C1-L1) data via the LCI. However, the Landsat Collection 2 data distribution process was start on December in 2020, and this data improvements for the geometric and radiometric quality (Wulder, 2019). The Landsat Collection 2 Level-1 (C2-L1) data are processed based on data quality and level of processing of the previous Landsat C1-L1 data and the data has fully compatibilities. However, the Landsat Collection 1 data will end on December 31, 2022. From the above, we investigated the effects of differences in the Landsat Collection Levels between the C1-L1 data and the C2-L1 data on estimation of the Chl.a concentration ion via the LCI.

2. DATA

In this study, we targeted around of the Yura Peninsula at the Uwa Sea located of Uwajima City and Ainan Town of Ehime Prefecture in Japan, where a pearl farming is conducted. The target area was shown in Figure 1 on the Sea Surface Temperature image of Landsat-8/TIRS acquired on July 13th, 2017. As a satellite data, we used five scene of Landsat-8/OLI data observed over the Uwa Sea (Path-Row: 112-037) in 2017 were used to compute the LCI. Here we collected the both collections data (C1-L1 and C2-L1) of the same day respectively. On the other hand, as a reference value of the Chl.a concentration (at depth 0 m), we used three water quality survey results measured at 4 locations in Uwajima City in 2017 and three water quality survey results measured at 2 locations in Utsumi of Ainan Town in 2017 were used. A list of acquisition dates of Landsat-8/OLI data and those of the water quality survey data was shown in Table 1.

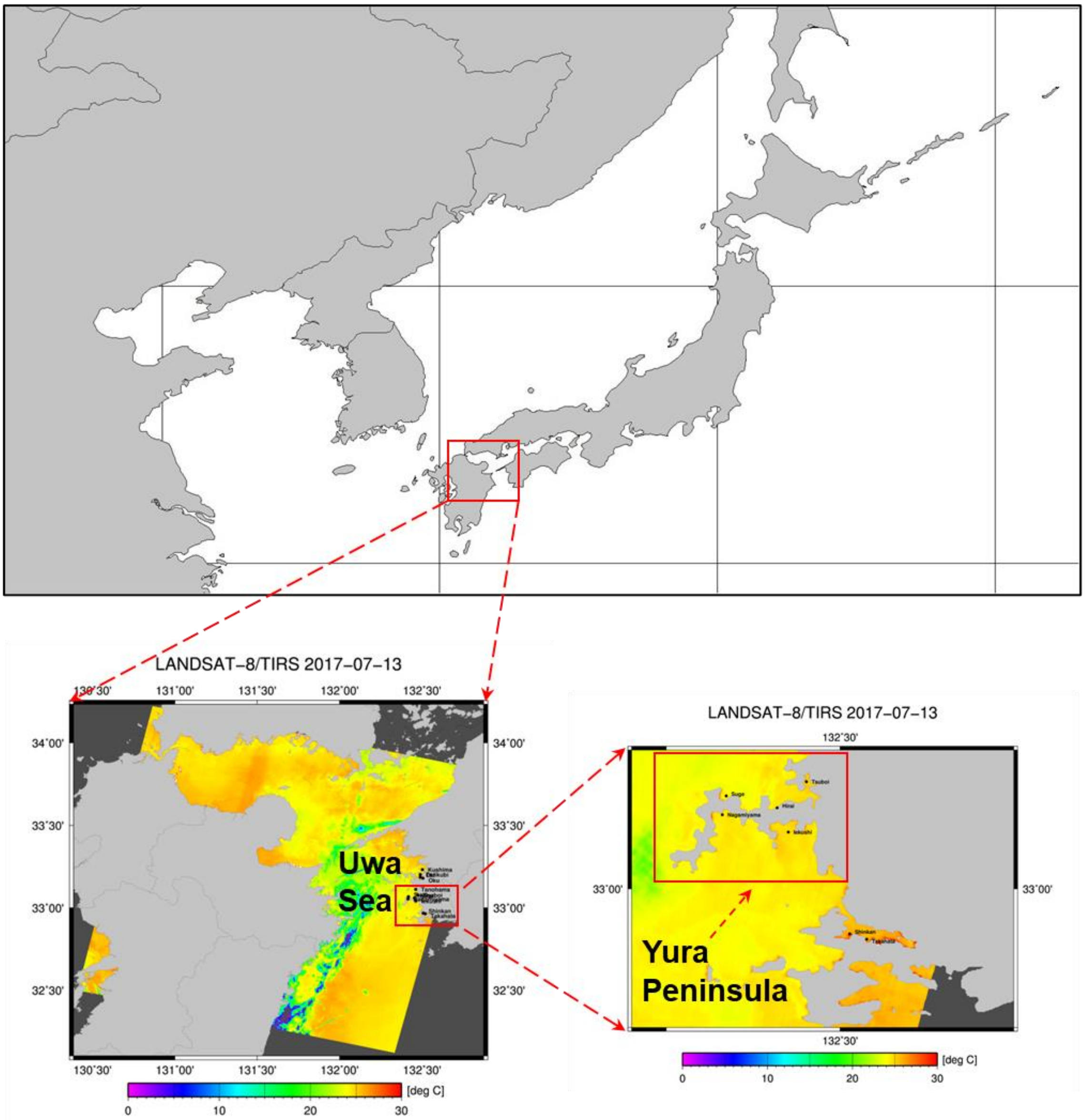

Figure 1. The target area of around of the Yura Peninsula at the Uwa Sea (Uwajima City and Utsumi of Ainan Town of Ehime Prefecture in Japan).

Table 1. A list of acquisition dates of Landsat-8/OLI data and those of the water quality survey data.

Landsat-8/OLI Path-Row: 112-037	Water quality survey around of the Yura Peninsula at theUwa Sea	
	Around Uwajima City	Around Ainan Town
2017/05/26	2017/05/11	2017/05/18
2017/07/13	2017/07/20	2017/07/18
2017/07/29		
2017/08/30	2017/09/11	-
2017/11/02	-	2017/11/16

3. METHOD

The LCI proposed by Robert Frouin (2006) is defined as the sum of the 3 or 4 bands of the aerosol reflectance $Ra(\lambda_i)$ and the water reflectance $Rw\,(\lambda_i)$ as follows:

$$\text{LCI} = \sum_{i=1}^{k} a_i R_a\,(\lambda_i) + \sum_{i=1}^{k} a_i\, R_w(\lambda_i)\,, \tag{1}$$

where to eliminate most of the atmospheric influence on the LCI, we approximate the aerosol reflectance $Ra(\lambda_i)$ as a function of wavelength λ_i and set the sum of $a_iRa(\lambda_i)$ to zero.
That is, the sum of $a_iRa(\lambda_i)$ on the first term of Eq. (1) replaces as follows:

$$\sum_{i=1}^{k} a_i R_a\,(\lambda_i) \approx \sum_{i=1}^{k} a_i \lambda_i^{\eta_j} = 0. \tag{2}$$

Consequently, the LCI of Eq. (1) is rewritten as follows:

$$\text{LCI} \approx \sum_{i=1}^{k} a_i\, R_w(\lambda_i). \tag{3}$$

In additions Eq. (2) and Eq. (3) were solved by the following four steps procedure.

Step 1: The wavelength λ_i are assumed the following Landsa-8/OLI bands: (1) band 1 (443 nm) which is the absorption band of the Chl.a, (2) band 2 (483 nm) which is the absorption band of the Chl.b, (3) band 3 (561 nm) which is a non-absorption band of the Chl.a and the Chl.b, (4) band 4 (655 nm) which is also a non-absorption band of the Chl.a and the Chl.b, and (5) band 5 (864 nm) which is the indicating aerosol effect. From these five bands, as the four-band combinations (k=4) that includes either band 1 or band 2, or both, we assumed the follows five cases: (1) bands 1, 2, 3 and 4, (2) bands 1, 2, 3 and 5, (3) bands 1, 2, 4 and 5, (4) bands 1, 3, 4 and 5, and (5) bands 2, 3, 4 and 5. From our previous study, it was confirmed that for the case of four-bands combinations, (1) bands 1, 2, 3 and 4, (2) bands 1, 2, 3 and 5, (3) bands 1, 2, 4 and 5 indicated the coefficients of determination R^2 greater than 0.5. Moreover, it was also confirmed that the coefficients of determination R^2 of the band combinations 1, 2, 3 and 5 was the highest with 0.811 (Oguro, 2021). The above-mentioned reasons, we fixed to the four-band combinations (k=4) of 1, 2, 3, and 5 in the following analysis.

Step 2: We approximated the exponent η_j in Eq.(2) with the normalized reflectance of sand, clouds and water. Here, for sand and water, we measured the reflectance in our laboratory. After that, the measured reflectance were divided by the maximum value of reflectance to obtain the normalized reflectance, respectively. On the other hand, we assumed a perfect white cloud and assumed the normalized reflectance of 1.0 regardless of wavelength since it is difficult to uniformly determine the normalized reflectance of clouds. The normalized reflectance of sand, clouds and water in the case of four-band combinations 1, 2, 3 and 5 were shown in Figure 2.

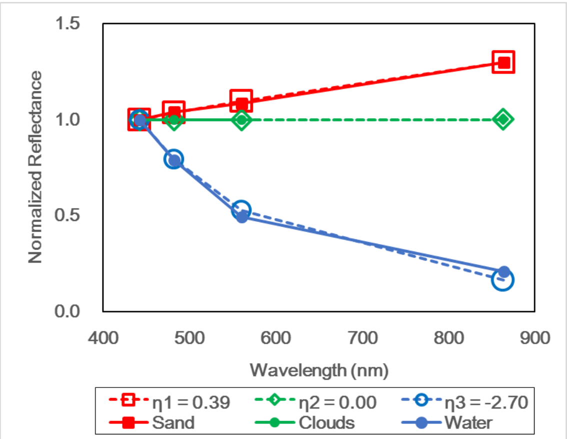

Figure 2. Normalized reflectance of sand, clouds and water in the case of four-band combinations 1, 2, 3 and 5.

Step 3: For the easier calculation the coefficient a_1 of the shortest wavelength band was fixed to 1, and the remaining coefficients of a_2, a_3 and a_5 were solved by the simultaneous linear equation. The Eq. (4) showed the case of band combinations of 1, 2, 3 and 5 for $\eta_1=0.39$, $\eta_2=0.00$ and $\eta_3=-2.70$.

$$\begin{cases} a_1\lambda_1^{0.39} + a_2\lambda_2^{0.39} + a_3\lambda_3^{0.39} + a_5\lambda_5^{0.39} = 0, \\ a_1\lambda_1^{0.00} + a_2\lambda_2^{0.00} + a_3\lambda_3^{0.00} + a_5\lambda_5^{0.00} = 0, \\ a_1\lambda_1^{-2.70} + a_2\lambda_2^{-2.70} + a_3\lambda_3^{-2.70} + a_5\lambda_5^{-2.70} = 0, \end{cases} \tag{4}$$

where the coefficient a_2, a_3 and a_5 were solved as -1.9692, 1.0984 and 0.1292, respectively.

Step 4: The LCI of Eq. (3) was solved as Eq. (5) in the case of four-band combinations of 1, 2, 3 and 5.

$$LCI \approx R_w(\lambda_1) - 1.9692R_w(\lambda_2) + 1.0984R_w(\lambda_3) - 0.1292R_w(\lambda_5). \tag{5}$$

4. RESULTS

4.1 Results of survey Data

In the area around of the Yura Peninsula at the Uwa Sea located of Uwajima City and Ainan Town of Ehime Prefecture in Japan, we compared the LCI in the case of four-band combinations 1, 2, 3 and 5 calculated from Landsat-8/OLI data of the Collection 1 and the Collection 2, and the Chl.a concentration based on the water quality survey (at depth 0 m). After that, the relation between calculated LCI and survey Chl.a concentration was approximated by exponential function. The results of the Collection 1 and the Collection 2 were shown in Figure 3(a) and Figure 3(b), respectively. Moreover, the Chl.a estimation formulas of those were shown in Eq. (6) and Eq.(7), respectively. Here, the resulted coefficients of determination R^2 were very low as 0.4535 and 0.4404, respectively since the range of the Chl.a concentrations based on the water quality survey was from 0.37 through 1.33 (mg/m^3).

$$Chl.a \approx 2.0414\ exp(129.1657\ LCI). \tag{6}$$

$$Chl.a \approx 2.1728\ exp(130.1658\ LCI). \tag{7}$$

4.2 Results of simulated Data

In this section, we simulated the spectral reflectance for the Chl.a concentrations ranging from 0.1 through 10 (mg/m^3) using the Bio-optical model of oceanic water by Morel (1988 and 2001) since the range of the Chl.a concentrations based on the water quality survey was very narrow ranging from 0.37 through 1.33 (mg/m^3). Here, the simulated the spectral reflectance for the range of wavelength from 350 through 700 nm were shown in Figure 4. From these spectral reflectance, we calculated the LCI in Eq.(5) for the Chl.a concentrations ranging from 0.1 through 10 (mg/m^3).

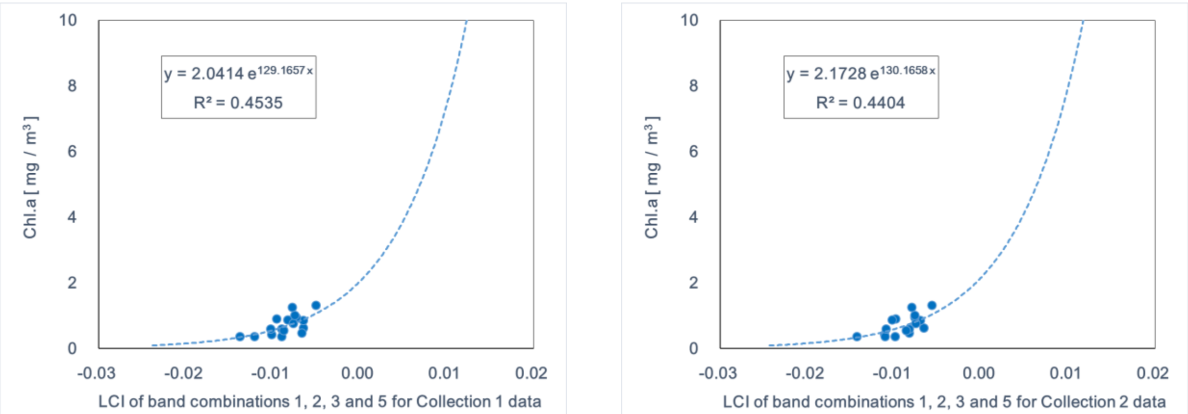

(a) Collection 1 (b) Collection 2

Figure 3. Relation between the calculated LCI and survey Chl.a concentration in the case of four-band combinations 1, 2, 3 and 5 of Landsat-8/OLI data for the Collection 1 and the Collection 2.

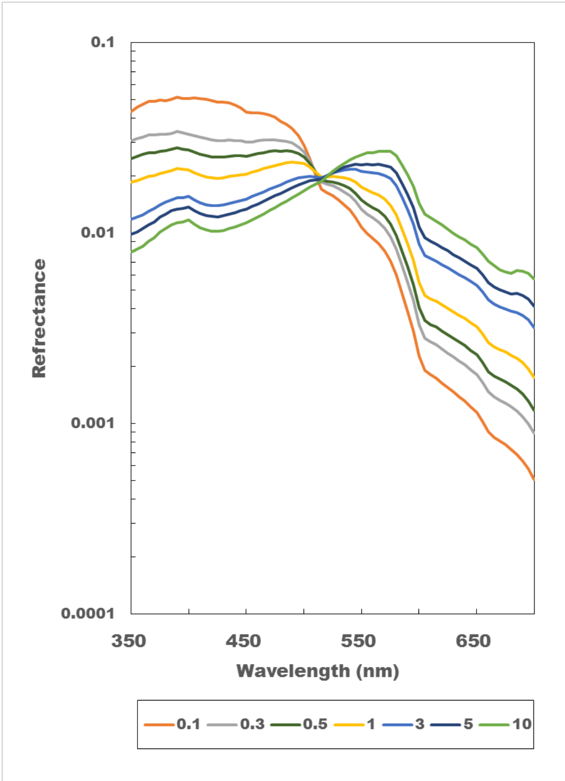

Figure 4. Simulated spectral reflectance for the Chl.a concentrations ranging from 0.1 through 10 (mg/m^3) by the Bio-optical model by Morel (1988 and 2001).

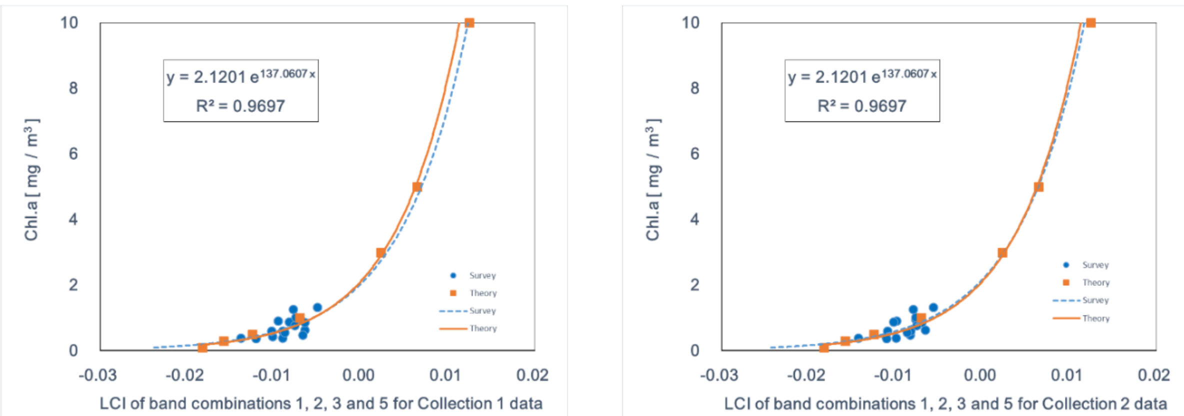

(a) Collection 1 (b) Collection 2

Figure 5. Relation between the calculated LCI and simulated Chl.a concentration in the case of four-band combinations 1, 2, 3 and 5 of Landsat-8/OLI data for the Collection 1 and the Collection 2 (overlaid on Figure 3).

After that, the relation between calculated LCI and simulated Chl.a concentration was approximated by exponential function. The results of the Collection 1 and the Collection 2 were shown in Figure 5(a) and Figure 5(b), respectively. Moreover, the Chl.a estimation formula was shown in Eq. (8). Here, the resulted coefficients of determination R^2 was very high as 0.9697. From Figure 5(a) and Figure 5(b), the simulated result was matched to the case of the Collection 2 than the case of the Collection 1. Moreover, we confirmed that the root-mean-squared (RMS) error of 12.4% and 9.4% in the range of Chlorophyll-a concentration 0.3–10 mg/m^3 for the C1-L1 data and C2-L1 data, respectively.

$$Chl.a \approx 2.1201\ exp(137.0607\ LCI). \quad (8)$$

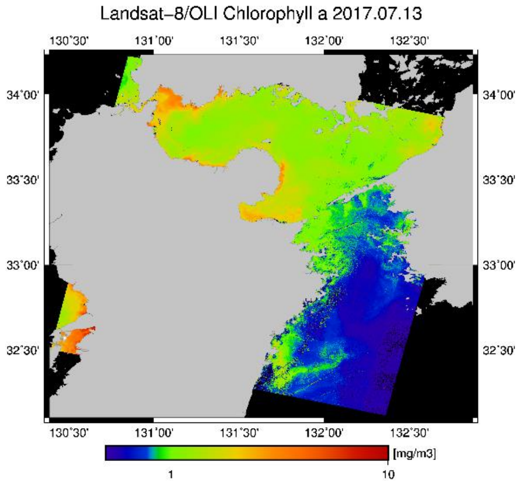

(a) Collection 1

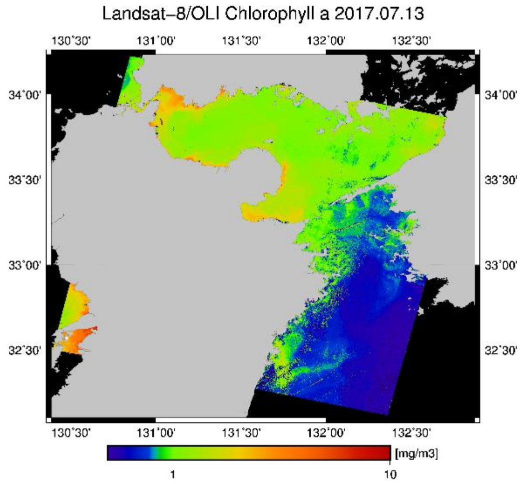

(b) Collection 2

Figure 6. Example of the calculated Chl.a concentration in the case of four-band combinations 1, 2, 3 and 5 of Landsat-8/OLI data for the Collection 1 and the Collection 2 on July 13th, 2017.

4.3 Results of Calculated Chl.a Concentration Images

As an example, the calculated Chl.a concentration in the case of four-band combinations 1, 2, 3 and 5 of Landsat-8/OLI data for the Collection 1and the Collection 2 on July 13th, 2017, was shown in Figure 6. From Figure 6(a) and Figure 6(b), the distribution pattern of the Chl.a concentration showed almost the same features. However, the Collection 2 image had slightly higher Chl.a concentration than the Collection 1 image. The Collection 2 seems to be more sensitive to slight changes in the LCI since the coefficient and the exponent of the exponential function of Eq.(7) of the Collection 2 were slightly larger than those in Eq.(6) of the Collection 1.

5. CONCLUSIONS

In this paper, we investigated the effects of differences in Landsat Collection Levels between the Collection 1 Level-1 data and the Collection 2 Level-1 data on calculated of Chl.a concentration via the LCI. From the above-mentioned analysis, it was clarified that the following:

- From the results of survey data, the resulted coefficients of determination R^2 were very low as 0.4535 and 0.4404, respectively since the range of the Chl.a concentrations based on the water quality survey was from 0.37 through 1.33 (mg/m^3).

- From the results of simulated data, the resulted coefficients of determination R^2 was very high as 0.9697. The simulated result was exactly fitted with the case of the Collection 2 in Eq.(7) than the case of the Collection 1 in Eq.(6) since the accuracy of the absolute geometry collection was substantial improvement by the global ground reference dataset.

- From the results of calculated Chl.a concentration images, the distribution pattern of Chl.a concentration showed almost the same features. However, the Collection 2 image had slightly higher Chl.a concentration than the Collection 1 image. The Collection 2 seems to be more sensitive to slight changes in LCI since the coefficient and the exponent of the exponential function of the Collection 2 were slightly larger than those of the Collection 1.

Here, the water quality survey in this analysis was not a fully simultaneous observation with Landsat-8/OLI. As the future works, we will perform the measurement of Chl.a concentration simultaneously with a satellite observation and we will verify this analysis.

REFERENCES

Frouin, R., Deschamps, P., Gross-Colzy, L., Murakami, H., and Nakajima, T., 2006. Retrieval of Chlorophyll-a Concentration via Linear Combination of ADEOS-II Global Imager data. Journal of Oceanography, 62 (3), pp. 331-337.

Morel, A., 1988. Optical Modeling of Upper Ocean in Relation to Its Biogenous Matter Content (Case I waters), Journal of Geophysical Research, 93 (C9), pp.10749-10768.

Morel, A. and Maritorena, S., 2001. Bio-optical properties of oceanic waters: A reappraisal, Journal of Geophysical Research, 106 (C4), pp.7163-7180.

Oguro, Y., Konishi, T., Ito, S. and Miura, C., 2021. An Estimation Method of Appropriate Chlorophyll-a Concentrations via Linear Combination Index for Landsat-8/OLI Data in Hiroshima Bay, International Symposium on Remote Sensing 2021, pp. 87-90.

Sakuno, Y., Makio, K., Koike, K., Maung-Saw-Htoo-Thaw, Kitahara, S., 2013. Chlorophyll-a Estimation in Tachibana Bay by Data Fusion of GOCI and MODIS Using Linear Combination Index Algorithm. Advances in Remote Sensing, 2, pp.292-296.

Wulder, M.A., Loveland, T.R., Roy, D.P., Crawford, C.J., Masek, J.G., Woodcock, C.E., Allen, R.G., Anderson, M.C., Belward, A.S., et al., 2019. Current status of Landsat program, science, and applications: Remote Sensing of Environment, v. 225, p. 127–147.